Title
Innovative C 2 -symmetric testosterone and androstenedione dimers: Design, synthesis, biological evaluation on prostate cancer cell lines and binding study to recombinant CYP3A4

Authors
Paquin, Alexis
Oufqir, Yassine
Sevrioukova, Irina F
et al.

Publication Date
2021-08-01

DOI
10.1016/j.ejmech.2021.113496

Peer reviewed

HHS Public Access

Author manuscript

Eur J Med Chem. Author manuscript; available in PMC 2022 August 05.

Published in final edited form as:

Eur J Med Chem. 2021 August 05; 220: 113496. doi:10.1016/j.ejmech.2021.113496.

Innovative C_2-symmetric testosterone and androstenedione dimers: Design, synthesis, biological evaluation on prostate cancer cell lines and binding study to recombinant CYP3A4

Alexis Paquin[a,c], **Yassine Oufqir**[b,c], **Irina F. Sevrioukova**[d], **Carlos Reyes-Moreno**[b,c], **Gervais Bérubé**[a,c,*]

[a]Département de Chimie, Biochimie et Physique, Université Du Québec à Trois-Rivières, C.P. 500, Trois-Rivières, QC, G9A 5H7, Canada

[b]Département de Biologie Médicale, Université Du Québec à Trois-Rivières, C.P. 500, Trois-Rivières, QC, G9A 5H7, Canada

[c]Groupe de Recherche en Signalisation Cellulaire, Université Du Québec à Trois-Rivières, C.P. 500, Trois-Rivières, QC, G9A 5H7, Canada

[d]Department of Molecular Biology and Biochemistry, University of California, Irvine, CA, 92697, United States

Abstract

The synthesis of two isomeric testosterone dimers and an androstenedione dimer is reported. The design takes advantage of an efficient transformation of testosterone leading to the synthesis of the key diene, 7α-(buta-1,3-dienyl)-4-androsten-17β-ol-3-one, through an elimination reaction. It was found that in some instances the same reaction led to partial epimerization of the 17β-hydroxyl group into the 17α-hydroxyl group. The specific orientation of the hydroxyl function was confirmed by NMR spectroscopy. Capitalizing on this unforeseen side reaction, several dimers were assembled using an olefin metathesis reaction with Hoveyda-Grubbs catalyst. This led to the formation of two isomeric testosterone dimers with 17α-OH or 17β-OH (**14α** and **14β**) as well as an androstenedione dimer (**14**). The new dimers and their respective precursors were tested on androgen-dependent (LNCaP) and androgen independent (PC3 and DU145) prostate cancer cells. It was discovered that the most active dimer was made of the natural hormone testosterone (**14β**) with an average IC_{50} of 13.3 μM. In LNCaP cells, **14β** was ~5 times more active than the antiandrogen drug cyproterone acetate (IC_{50} of 12.0 μM vs. 59.6 μM, respectively). At low concentrations (0.25–0.5 μM), **14α** and **14β** were able to completely inhibit LNCaP cell growth induced by testosterone or dihydrotestosterone. Furthermore, cross-reactivity of androgen-based

*Corresponding author. Département de Chimie, Biochimie et Physique, Université Du Québec à Trois-Rivières, C.P. 500, Trois-Rivières, QC, G9A 5H7, Canada. Gervais.Berube@uqtr.ca (G. Bérubeé).

Declaration of competing interest

The authors declare that they have no known competing financial interests or personal relationships that could have appeared to influence the work reported in this paper.

Appendix A. Supplementary data

Supplementary data to this article can be found online at https://doi.org/10.1016/j.ejmech.2021.113496.

dimers with sterol-metabolizing cytochrome P450 3A4 was explored and the results are disclosed herein.

Keywords

Androstenedione; Cancer; CYP3A4; Dihydrotestosterone; Dimers; Testosterone

1. Introduction

Modern chemistry along with the refinement of modern analytic methods and development of sensitive spectroscopic tools led to the discovery of important new chemical entities and medicines [1]. Hence, researchers continue to be captivated by ever more complex molecules. Amongst them, hybrid and dimeric molecules are subject to significant scrutiny by scientists [2-9]. This manuscript reports the design and synthesis of steroid dimers as prospective “natural antiandrogens” for the treatment of prostate cancer (PCa). It is well known that steroid receptors dimerize upon interaction with their cognate hormones. This biological response occurs for the androgen receptor (AR) upon its binding with the androgens, testosterone (TS) and dihydrotestosterone (DHT). Dimerization of AR was shown to proceed via the ligand-binding domain and is induced by receptor agonists but not antagonists [10]. Hence, the design of a steroid-based antiandrogen might be key for the discovery of new therapeutics and for studying the AR, as well as other important biological macromolecules involved in sterol metabolism, such as cytochrome P450 3A4 (CYP3A4) [11,12].

Several examples of TS (**1**) and androstenedione (**2**) dimers are already described in the literature (Fig. 1). Some compounds, such as the dimeric silyl ethers **3** and **4** and the oxalate dimer **5**, were designed to act as prodrugs of TS in animal models [13,14]. Alternatively, dimers **6a-d** and **7a-c** linked by the aliphatic or aromatic chains, respectively, were made to work as possible antiandrogens [15]. Androstenedione (**2**) was also derivatized to the thioether dimer **8** and the trithiolane dimer **9** [16]. The latter compound exhibited antifungal activity against *Saccharomyces cerevisi* [17]. We have also investigated the synthesis and biological potential of two isomeric TS dimers, *cis*-**10** and *trans*-**10** (Fig. 2) [11]. The MTT antiproliferative assay showed that the *cis* isomer was as active as CPA, with IC_{50} of 30.3 μM and 24.7 μM on LNCaP (AR+) and PC3 (AR^{-}) PCa cells, respectively. In addition, these two molecules were used to study allosteric effects in substrate binding to CYP3A4 by spectroscopic methods [12]. It was discovered that *cis*-**10** binds to CYP3A4 stronger and causes more pronounced conformational changes in the ferric and Fe^{2+}-CO states.

In Canada, the lung, breast, colorectal and prostate cancers are most prevalent, with roughly 107,700 new cases estimated in 2020 [18]. This is ~48% of all new cancer cases, where PCa alone represents one fifth. Among the estimated 23,300 new cases in men, 18% will be lethal. Thus, PCa is still the most common cancer in men [18] and can be cured successfully only if detected at an early stage. Nevertheless, new therapeutics are persistently sought by many research teams to fight this disease. The vast majority of malignancies are detected at stage I or II and classified as hormone-dependent [18,19]. Hence, it is conceivable to use the

AR as a biological target to design site-specific antiandrogens for treatment of PCa. Herein, we report the synthesis and properties of three new androgen-based dimers linked by an α,ω-hexatrienyl chain at carbon 7 of the steroid nucleus. We also report on their binging interactions with CYP3A4.

2. Design and chemistry

TS and DHT are natural substrates for the AR [10]. Hence, if transformed adequately, they can be used as carrier molecules to target prostate tissue via AR activation or inactivation. Capitalizing on our earlier work, the 7α position of TS was selected for dimer linkage, as it is suitably located away from the important binding sites, namely the 3-C═O and 17-OH groups, crucial for hydrogen bonding with AR [11,15]. These two key functional groups must remain intact to promote strong interactions with the receptor [11].

The synthetic methodology for the preparation of new dimers is described in Scheme 1. As reported earlier, TS was efficiently modified by a five-step reaction sequence into the intermediate 7α-allyl-4-androstene-17β-ol-3-one acetate (**11**) [11]. The 7α-(4-chloro-but-2-enyl)-4-androsten-17β-ol-3-one intermediate (**12**) was obtained from TS using the Hoveyda-Grubbs metathesis reaction with allyl chloride, giving 41% overall yield [20]. Afterwards, treatment of **12** with a mixture of cesium carbonate and the ruthenium catalyst led to formation of the key intermediate, 7α-(buta-1,3-dienyl)-4-androsten-17β-ol-3-one (**13β**), with 66% yield [21]. Upon treatment with the Hoveyda-Grubbs catalyst, the latter derivative gave 63% of the TS dimer **14β**. Similarly, using a different lot of the ruthenium catalyst, a mixture of **13β** and **13α** isomeric dienes was obtained in 17% and 18% yield, respectively. Stereochemistry of **13β** (a TS derivative) and **13α** (an epitestosterone (epiTS) derivative) was easily confirmed by comparison of the ^{13}C NMR chemical shift of the angular 18-CH_3 group on the estrogenic steroid nucleus. It is reported that the angular 18-CH_3 chemical shift for 17β- and 17α-estradiol molecules is 11.68 ppm and 17.61 ppm, respectively [22]. Similarly, we observed the angular 18-CH_3 chemical shifts of 11.0 ppm and 16.9 ppm for **13β** and **13α**, respectively, confirming the stereochemistry of the 17-OH group on the TS nucleus. Also by ^{13}C NMR, the 17-C was located at 81.3 ppm and at 79.5 ppm for the **13β** and **13α** isomers, respectively. The ^{1}H NMR 17-CH signal appears at 3.62 ppm as a triplet for **13β** and at 3.73 ppm as a doublet for **13α**, further confirming the stereochemistry at 17-C.

Even though the epimerization was a surprising side reaction, it was decided to take advantage of this result and produce the epiTS dimer **14α** for comparative analysis with the "natural" TS dimer **14β** and the androstenedione dimer **14**. The precursor **13** for the synthesis of androstenedione dimer was obtained by oxidation of the 7α-(buta-1,3-dienyl)-4-androsten-17β-ol-3-one (**13α/β**) isomer mixture with pyridinium chlorochromate on alumina in dichloromethane with 63% yield [23]. Again, the synthesis of dimers **14α** and **14** was performed using a metathesis reaction condition and the 2nd generation Hoveday-Grubbs catalyst with 34% and 77% yield, respectively [24,25]. In order to further characterize the diene **13β**, a Diels-Alder reaction was performed with maleic anhydride in toluene at reflux to yield 19% of the adduct **15** (Scheme 2) [26]. All new molecules were

fully characterized by infrared (IR) and nuclear magnetic resonance (^{1}H and ^{13}C NMR) spectroscopy and by high-resolution mass spectrometry (HRMS) analyses.

3. Results and discussion

3.1. Antiproliferative activity of new compounds on prostate cancer cell lines

The antiproliferative activity of compounds **13, 13α, 13β, 14, 14α, 14β** and **15** was measured using the MTT assay on three PCa cell lines: LNCaP (AR+), PC3 (AR−) and DU145 (AR−) [27,28]. The antiandrogen drug cyproterone acetate (CPA) was used as a positive control to better contrast the biological activity of new steroid dimers and their respective precursors. The results from the antiproliferative activity assay are presented in Table 1, where IC_{50} is the compound concentration inhibiting cell growth by 50%.

The results show that the diene precursors **13, 13α, 13β** were generally more active than CPA on all tested PCa cells. For instance, their IC_{50} was in the 16.6–33.5 μM range vs. 59.6 μM for CPA on LNCaP (AR+) cells. On PC3 (AR−) cells, IC_{50}s varied from 31.5 μM to μM relative to 56.9 μM for the reference drug, and from 21.3 μM to 29.0 μM vs. 50.7 μM on the AR− DU145 cells (Table 1). The best diene precursor was **13α** with IC_{50} of 16.6 μM, which is about 4 times lower than that for CPA on the LNCaP AR + cells. The two TS dimers, **14α** and **14β**, displayed most interesting biological results. The **14β** dimer was the most potent inhibitor on all cells tested, with IC_{50} of 12.0, 13.6 and 14.4 μM on LNCaP, PC3 and DU145 cell lines, respectively. Moreover, **14β** was about 5 times more active than CPA on LNCaP cells. The epiTS dimer **14α** was less active than **14β**, with IC_{50} varying from 21.4 μM to 44.5 μM on different cell lines. Likewise, the androstenedione dimer **14** had IC_{50} in the 29.0–72.7 μM range. The Diels-Alder adduct **15** was the least active compound, with IC_{50} ranging from 62.5 μM to 130.6 μM on all PCa cells tested. We were surprised to observe no obvious selective activity of the best dimer **14β** on the AR + PCa cells (Table 1). Nevertheless, it is known that there are often some discrepancies between *in vitro* and *in vivo* experiments [29,30], so **14β** could potentially show better selectivity in *in vivo* settings.

3.2. Antiandrogenic potential of testosterone dimer (14β) and epitestosterone dimer (14α)

The antiandrogenic potential of **14β** and **14α** was evaluated *in vitro* by monitoring the inhibition of cell proliferation induced by TS and DHT in LNCaP (AR+) PCa cells. The results are shown in Figs. 3 and 4. We were able to demonstrate in a competitive assay that both the TS dimer **14β** and the epiTS dimer **14α** were able to fully inhibit the proliferative effect induced by 0.1 nM TS or DHT on LNCaP (AR+) PCa cells (Figs. 3 and 4). Cell growth stimulation by TS and DHT alone (black bars) led to about 1.39 and 1.41 fold induction, respectively, compared to the control cells treated with 0.1% dimethyl sulfoxide (DMSO) in culture media (relative cell proliferation = 1). For the TS-induced cell proliferation, the dimers **14α** and **14β** were 100% effective at a concentration of 0.25 μM and 0.5 μM, respectively (Fig. 3). Of note, at 1 μM concentration, **14α** and **14β** reduced TS-induced cell proliferation to 84% and 98% of the initial (non-stimulated) level, respectively (Fig. 3). Relative to the proliferative response induced by 0.1 nM TS, the reduction was ~141% and 104%, respectively. In contrast, for the DHT-induced cell proliferation, both dimers were 100% effective at a concentration of 1 μM (Fig. 4). It is important to indicate

that (i) even at 0.125 μM concentration both dimers were able to inhibit at least 45% of the growth induced by TS and DHT; (ii) under these conditions **14α** inhibited 82% of LNCaP cell growth induced by TS; and (iii) the effective concentration levels (0.125 μM–1 μM) were well below the IC_{50}s of the dimers on LNCaP cells (see Table 1). However, it should be mentioned that the pronounced inhibitory effect of **14α** and **14β** observed at 1 μM concentration might be due to their dual anti-proliferative and anti-androgenic actions. As Fig. 5 shows, **14α** and, to a larger extent, **14β** display higher cytocidal activity on LNCaP cells than CPA within a wide concentration range.

3.3. Interaction of steroid dimers with recombinant CYP3A4

Androgens and androgen receptor signaling regulate prostate growth/homeostasis and play a crucial role in prostate cancer pathogenesis. Systemic androgen levels are maintained through *de novo* synthesis and metabolism. One important enzyme participating in steroid metabolism is CYP3A4, which oxidizes TS, androstenedione and DHT to biologically less active derivatives [31,32]. Moreover, there is experimental evidence that CYP3A4 can simultaneously bind multiple sterol molecules [12,33]. Therefore, it was of interest to investigate whether the TS dimers (**14α** and **14β**) and androstenedione dimer (**14**) can bind to and alter the functional activity of CYP3A4.

Binding affinity and inhibitory potency for CYP3A4—Spectral measurements showed that all three compounds could approach the heme and cause a partial blue shift in the Soret band (type I spectral change), indicative of a low-to-high spin transition (Fig. 6). The estimated dissociation constant (K_d) for **14α** and **14** was similar (1.6 and 1.4 μM, respectively) and ~4-fold lower than for **14β** (Table 2). The dimers also inhibited the functional activity of CYP3A4, albeit to a different extent. The IC_{50} values for the 7-benzyloxy-4-(trifluoromethyl)coumarin (BFC) debenzylase activity measured in a soluble reconstituted system varied by an order of magnitude: from 1.2 μM for **14β** to 22 μM for **14α**, with no correlation with the respective K_d values. This is in contrast to the previously reported *cis*-**10** and *trans*-**10** dimers, whose IC_{50} and K_d correlated well (Table 2). As observed for the nanodisc-incorporated CYP3A4 [12], *cis*-**10** was found to bind tightly and induced a nearly complete high spin shift in isolated CYP3A4 (Fig. S1). The high spin content in *trans*-**10** bound CYP3A4 was only 65%, which is still considerably higher than in the **14α-, 14β-** and **14**-bound forms (Table 2). It should be noted that the K_d values for *cis*-**10** and *trans*-**10** derived for the soluble and membranous CYP3A4 [12] were highly similar, meaning that the lipid bilayer had no feasible effect on the binding affinity.

Overall, *cis*-**10** was the strongest binder and inhibitor of CYP3A4. **14β** had a comparable IC_{50}, whereas **14** and **14α** displayed the intermediate and the lowest inhibitory potency, respectively. This implies that **14α** should have the lowest impact on CYP3A4-dependent androgen metabolism in *cellulo* and *in vivo*. In addition to the adult liver and intestines, where CYP3A4 is predominantly expressed, it has been detected at a transcript and protein level in prostate tissue, where decreased expression of CYP3A4 is associated with poorer cancer-specific survival [34,35]. None of the tested PCa cell lines appreciably express CYP3A4 and, thus, the inhibitory ability of sterol dimers is unlikely to interfere with the cell proliferation assays (Figs. 3 and 4). However, because the dimer concentrations used in the

latter assays (up to 1 μM) and some of the IC_{50} values for CYP3A4 (Table 2) are comparable, the possibility that the dimers could cross-react with CYP3A4 and alter androgen metabolism exists and should be taken into account during further evaluation.

Crystal structure of CYP3A4 bound to cis-10—To obtain direct insights on the interaction of CYP3A4 with sterol dimers, we attempted to crystallize various complexes but succeeded only in solving the CYP3A4-*cis*-**10** structure to 2.75 Å resolution (Table S1). In the crystal structure, *cis*-**10** is bound to the active site above the cofactor (Fig. 7). The sterol moiety closest to the heme is well defined and H-bonds to Ala305 carbonyl via the hydroxyl group, while the opposite keto group forms weak electrostatic interactions with the Glu374 side chain. Comparison with the water-bound CYP3A4 structure (4I3Q; 2.6 Å) showed that the binding of *cis*-**10** imposes spatial constraints, forcing the I-helix to move aside and the heme plane tilt to downside by 1.2 and 0.7 Å, respectively (Fig. 8). In addition to the vertical shift, the heme cofactor has a slightly altered conformation of the vinyl groups (Fig. 8B). This supports the resonance Raman spectroscopy results, which also indicate that association of CYP3A4 with *cis*-**10** leads to conformational changes in the porphyrin side chains [12]. The second sterol ring is poorly defined, possibly due to multiple conformations, and imposes steric hindrance with the Phe108-centered loop, shifting aside by 2.9 Å, and with the F–F' connecting fragment, part of which (residues 211–215) becomes disordered. As a result, the active site expands and becomes more solvent accessible. Importantly, the proximal sterol faces the heme with the D ring (β-side) and its two carbon atoms, C16 and C18, are only 4.1 and 3.9 Å away from the heme iron (Fig. 7). This suggests that *cis*-**10** binds in a productive mode and could undergo oxidation. In contrast, TS approaches the heme with the A ring (β-side) of the steroid nucleus and undergoes oxidation primarily at C6β and C2β [36] and at the minor C1β and C11β sites [37,38], all of which are too far from the catalytic center in the crystal structure.

The main difference between *cis*-**10** and other dimer analogues is in the length and/or stereo configuration of the aliphatic linker, defining the relative positioning of sterol rings. Taking into account the big spread in *K*d and IC_{50} (Table 2) and the crystallographic binding mode of *cis*-**10** (Fig. 7), it is evident that both stereochemistry of the 17-OH and 3-C═O groups and spatial orientation of the distal sterol are important for the binding and inhibition of CYP3A4. The 17-OH and 3-C═O functionalities establish polar interactions that anchor the dimer to the active site, whereas the distal sterol could control the overall conformation and the access to the active site. As this study demonstrates, one way to modulate the inhibitory strength is to vary the linker length, which in turn, alters the dimer binding manner. Thus, the CYP3A4-*cis*-**10** complex provides the first insights on how monomeric and dimeric sterols can be oriented in the active site, supports the current and previous experimental findings, and helps better understand the underlying mechanism for the dimers' inhibitory action.

4. Conclusion

In this study, we prepared and characterized several androgen-based dimers designed for the treatment of PCa. The new molecules were tested on both AR+ and AR− PCa cells. It was discovered that the dimer made of the natural hormone TS, compound **14β**, was ~5 times

more active than the antiandrogen drug CPA and, along with the 17-OH stereoisomer **14α**, could completely inhibit TS or DHT stimulated LNCaP PCa cell growth at low concentrations. Both **14α** and **14β** could also bind and inhibit CYP3A4, the major androgen-metabolizing enzyme. Thus, further tests will be necessary to assess the potential impact of cross-reactivity with CYP3A4 and possible utilization of **14α** and **14β** as "natural antiandrogens" for PCa treatment.

5. Experimental protocols

5.1. Biological methods

The antiproliferative activity of all compounds was assessed using the 3-(4,5-dimethylthiazol-2-yl)-2,5-diphenyltetrazolium (MTT) assay [27,28]. LNCaP androgen-sensitive human prostate adenocarcinoma, PC3 androgen-insensitive human prostate adenocarcinoma and DU145 androgen-insensitive human prostate adenocarcinoma cells were purchased from the American Type Culture Collection (Manassas, VA). LNCap and PC3 were cultured in RPMI medium (Hyclone, Logan, UT) supplemented with 10% of calf serum and Penicillin-Streptomycin-Glutamine. The cells were maintained at 37 °C in a moisture saturated atmosphere containing 5% CO_2.

5.1.1. Antiproliferative activity assay—Cell viability of compounds **13, 13α, 13β, 14, 14α, 14β, 15** and CPA was determined by the MTT assay [27,28]. Briefly, 8×10^3 cells/well were seeded into 96-well plate and incubated overnight. After culturing for 48 h in fresh medium containing various concentrations of TS dimers, the cells were stained with MTT solution (0.5 mg/mL; Sigma-Aldrich) for 3 h at cell culture condition followed by dissolving with 10% Triton-X 100 in acidic isopropanol (0.1 N HCl). The cell growth was determined by measuring optical density (OD) value at 590 nm using the Synergy HT Microplate Reader (from Bio-Tek). Readings obtained from treated cells were compared with measurements of control cells plates fixed on the treatment day, and the percentage of cell growth inhibition was then calculated for each compound. Each condition included three replicate wells with three independent repeats.

5.1.2. Inhibition of testosterone- and dihydrotestosterone-induced cell proliferation of LNCaP PCa cells by dimers 14β and 14α—LNCaP cells were seeded at 8×10^3 cells/well into 96 well plates in medium as above supplemented with 10% FBS. After incubation for 48 h, the cells of the control group were treated with vehicle (DMSO, 0.1% in culture media), whereas the TS and DHT groups were treated at a concentration of 0.1 nM. The combination groups were also treated with 0.1 nM TS or DHT along with different concentrations of the dimers **14α** and **14β** (0.125, 0.25, 0.5 and 1 μM). After 48 h, the OD of the wells at 590 nm was measured using a microplate reader after incubation with MTT solution at 37 °C for 3 h as described above. Each condition included three replicate wells with three independent repeats.

5.2. Spectral and structural studies on CYP3A4

Codon-optimized full-length and Δ3-22 human CYP3A4 were produced as reported previously [39] and used for assays and crystallization, respectively. Equilibrium ligand

binding to CYP3A4 was monitored in a Cary 300 spectrophotometer at ambient temperature in 0.1 M phosphate buffer, pH 7.4, supplemented with 20% glycerol and 1 mM dithiothreitol. Sterol dimers were dissolved in DMSO and added to a 2 μM protein solution in small aliquots, with the final solvent concentration <2%. Spectral dissociation constant (K_d) was determined from hyperbolic or quadratic fits to titration plots. Inhibitory potency of sterol dimers for the BFC debenzylation activity of CYP3A4 was measured in a soluble reconstituted system as described in detail elsewhere [40]. CYP3A4 bound to *cis*-**10** was crystallized using a sitting drop vapor diffusion method. Prior to crystallization setup, CYP3A4 (60 mg/mL in 50 mM phosphate, pH 7.4) was incubated with a 5-fold excess of *cis*-**10** and centrifuged to remove the precipitate. The supernatant (0.5 μL) was mixed with 0.4 μL of crystallization solution containing 10% polyethylene glycol 3350 and 80 mM sodium malonate, pH 7.0. Crystals were grown at room temperature within 2 days and cryoprotected with Paratone-N before freezing in liquid nitrogen. X-ray diffraction data were collected at the Stanford Synchrotron Radiation Lightsource beamline 12–2. Crystal structure was solved by molecular replacement with PHASER [41] and 5VCC as a search model. The ligand was built with eLBOW [42] and manually fit into the density with COOT [43]. The initial model was rebuilt and refined with COOT and PHENIX. Polder omit electron density map was calculated with PHENIX. Data collection and refinement statistics are summarized in Table S1. The atomic coordinates and structure factors for the *cis*-**10**-CYP3A4 complex were deposited in the Protein Data Bank with the ID code 7LXL.

5.3. Chemistry

Anhydrous reactions were performed under an inert atmosphere of nitrogen. The starting material, reactant and solvents were obtained commercially and used as such or purified and dried by standard means [31,44]. Organic solutions were dried over magnesium sulfate ($MgSO_4$), filtered and evaporated on a rotary evaporator under reduced pressure. All reactions were monitored by UV fluorescence. Commercial TLC plates were Sigma T 6145 (polyester silica gel 60 Å, 0.25 mm). Flash column chromatography was performed according to the method of Still et al. on Merck grade 60 silica gel, 230–400 mesh [32,45]. All solvents used in chromatography were distilled prior to use.

The infrared spectra were taken on a Nicolet Impact 420 FT-IR spectrophotometer. Mass spectral assays were obtained using a MS model 6210, Agilent technology instrument. The high resolution mass spectra (HRMS) were obtained by TOF (time of flight) using ESI (electrospray ionization) using the positive mode (ESI+) (Université du Québec à Montréal and at Université Laval). Nuclear magnetic resonance (NMR) spectra were recorded on a Varian 200 MHz NMR apparatus. Samples were dissolved in deuterated chloroform ($CDCl_3$) for data acquisition using the residual solvent signal as internal standard (chloroform δ 7.26 ppm for ^{1}H NMR and δ 77.23 ppm for ^{13}C NMR). Chemical shifts (δ) are expressed in parts per million (ppm), the coupling constants (J) are expressed in hertz (Hz). Multiplicities are described by the following abbreviations: s for singlet, d for doublet, t for triplet and m for multiplet, and bs for broad singlet.

Note: The nomenclature of the TS derivatives described herein was based on the androgen skeleton (4-androsten-17β-ol-3-one) for clarity to the readers and to simplify the visualization of the molecules prepared in this manuscript.

5.3.1. Synthesis of testosterone and androstenedione dimers

5.3.1.1. Preparation of 7α-(buta-1,3-dienyl)-4-androsten-17β-ol-3-one (13β).: The precursor steroid 7α-(4-chloro-but-2-enyl)-4-androsten-17β-ol-3-one (**12**) (109 mg, 0.29 mmol) was dissolved in acetonitrile (3 mL) under a nitrogen atmosphere. To this solution was added cesium carbonate (375 mg, 1.15 mmol) and the ruthenium catalyst Ru(Cp*)$(MeCN)_3$] [PF6] (10.2 mg, 7% mol). The resulting mixture was stirred vigorously for two days at room temperature and in the dark (the reaction vessel was wrapped with aluminum paper). Afterwards, the reaction mixture was diluted with ether (100 mL), transferred into a separatory funnel and washed three times with water (3 × 75 mL). The organic phase was dried with anhydrous magnesium sulfate, filtered and evaporated under reduced pressure. The crude material was purified by flash chromatography (hexane/acetone, 9/1) to give 64.3 mg (66%) of the desired material. mp: 99–101 °C; IR ν (cm^{-1}): 3420 (O—H), 1651 (C═O), 1614 (C═C), 1238 (C—O); ^{1}H NMR (200 MHz, $CDCl_3$, δ ppm): 6.32–6.02 (2H, m, 21-CH and 22-CH), 5.72 (1H, s, 4-CH), 5.67–5.55 (1H, m, 20-CH) 5.17–5.00 (2H, m, 23-CH2), 3.62 (1H, t, J = 8.6 Hz, 17-CH), 1.23 (3H, s, 19-CH3), 0.79 (3H, s, 18-CH3); ^{13}C NMR (200 MHz, $CDCl_3$, δ ppm): 199.1 (C-3), 169.0 (C-5), 137.0 (C-20), 133.0 (C-22), 132.9 (C-21), 125.8 (C-4), 116.2 (C-23), 81.3 (C-17), 52.5, 47.1, 42.9, 41.1, 39.3, 39.0, 38.8, 36.0, 35.9, 34.0, 30.3, 22.7, 20.6, 17.8, 11.0; HRMS (ESI+): $(M + H)^+$ calculated for $C_{23}H_{33}O_2$ = 341.2475; found = 341.2475.

5.3.1.2. Preparation of 7α-(buta-1,3-dienyl)-4-androsten-17β-ol-3-one (13β) and 7α-(buta-1,3-dienyl)-4-androsten-17α-ol-3-one (13α).: As described above, the precursor steroid 7α-(4-chloro-but-2-enyl)-4-androsten-17β-ol-3-one (**12**) (499 mg, 1.32 mmol) was dissolved in acetonitrile (15 mL) under a nitrogen atmosphere. To this solution was added cesium (1.73 g, 5.29 mmol) and the ruthenium catalyst Ru(Cp*)$(MeCN)_3$] [PF6] (47 mg, 7% mol). The resulting mixture was stirred vigorously for two days at room temperature and in the dark (the reaction vessel was wrapped with aluminum paper). Afterwards, the reaction mixture was diluted with ether (500 mL), transferred into a separatory funnel and washed three times with water (3 × 375 mL). The organic phase was dried with anhydrous magnesium sulfate, filtered and evaporated under reduced pressure. The crude material was purified by flash chromatography (hexane/acetone, 9/1) to give 78.1 mg of **13β** (17%) along with 78.8 mg (18%) of the 17α-hydroxy isomer (**13α**). It is noteworthy to indicate that the latter product was usually not observed with this reaction. The epimerization of the hydroxyl function occurred only when a newly purchased ruthenium catalyst was used (lot #MKCK1977). 17β-hydroxy isomer **13β**: see section 4.2.1.1 for spectral data. 17α-hydroxy isomer **13α**: mp: 129–131 °C; IR ν (cm^{-1}): 3428 (O—H), 1660 (C═O), 1614 (C═C), 1225 (C—O). ^{1}H NMR (200 MHz, $CDCl_3$, δ ppm): 6.36–6.03 (2H, m, 21-CH and 22-CH), 5.72 (1H, s, 4-CH), 5,68–5,60 (1H, m, 20-CH) 5.14–4.97 (2H, m, 23-CH_2), 3,73 (1H, d, J = 5.9 Hz, 17-CH), 1.23 (3H, s, 19-CH_3), 0.70 (3H, s, 18-CH_3); ^{13}C NMR (200 MHz, $CDCl_3$, δ ppm): (C-3), 169.2 (C-5), 137.2 (C-20), 133.1 (C-22), 132.9 (C-21), 125.7 (C-4), 116.0 (C-23), 79.5 (C-17), 46.9, 45.3, 45.1, 41.8, 39.4, 39.3, 38.7, 35.9, 34.0, 32.4, 30.9, 24.0,

20.6, 17.8, 16.9; HRMS (ESI+): $(M + H)^+$ calculated for $C_{23}H_{33}O_2$ = 341.2475; found = 341.2472.

5.3.1.3. Preparation of 7α-(buta-1,3-dienyl)-4-androsten-3,17-dione (13).: The steroid 7α-(buta-1,3-dienyl)-4-androsten-17β-ol-3-one (**13α/β**) (18 mg, 0.05 mmol) was dissolved in methylene chloride (1 mL) and treated with pyridinium chlorochromate on alumina (33.8 mg, 0.16 mmol). The mixture was stirred at room temperature for 2.5 h. Afterwards, the reaction mixture was filtered on silica gel with methylene chloride as the eluent (30 mL) The organic phase was dried, filtered and evaporated to a brownish solid. The crude material was purified by flash chromatography (hexane/acetone, 9/1) to give 11.4 mg (65%) of the oxidized product **13**. mp: Decomposition begins at 163 °C; IR ν (cm^{-1}): 1734 (C═O), 1664 (C═O enone), 1615 (C═C); ^{1}H NMR (200 MHz, $CDCl_3$, δ ppm): 6.31–6.08 (2H, m, 21-CH and 22-CH), 5.75 (1H, s, 4-CH), 5.74–5.64 (1H, m, 20-CH) 5.18–5.01 (2H, m, 23-CH_2), 1.24 (3H, s, 19-CH_3), 0.91 (3H, s, 18-CH_3); ^{13}C NMR (200 MHz, $CDCl_3$, δ ppm): 220.0 (C-17), 198.9 (C-3), 168.1 (C-5), 136.7 (C-20), 133.4 (C-22), 132.2 (C-21), 126.0 (C-4), 116.7 (C-23), 47.6, 47.5, 47.1, 40.6, 39.3, 38.7, 38.5, 35.9, 35.5, 34.0, 30.9, 21.2, 20.3, 17.7, 13.7; HRMS (ESI+): $(M + H)^+$ calculated for $C_{23}H_{31}O_2$ = 339.2319; found = 339.2318.

5.3.1.4. Preparation of trans, trans,trans-1,6-bis-(17β-hydroxy-4-androsten-3-one-7α-yl)hexatriene (14β).: The steroid 7α-(buta-1,3-dienyl)-4-androsten-17β-ol-3-one (**13β**) (23.0 mg, 0.07 mmol) was dissolved in methylene chloride (0.5 mL). Under an inert atmosphere of nitrogen, a solution of 2nd generation Hoveyda-Grubbs catalyst (5.7 mg, 10% mol) in methylene chloride (0.5 mL) was added to the reaction mixture. The solution was stirred for 48 h in the dark. The nitrogen atmosphere was constantly purged during the first 2 h of the reaction, and if evaporation occurs the loss of the solvent was maintained throughout the reaction. Then, the reaction flask was regularly purged with nitrogen during the remaining course of the reaction. Afterwards, the solvent was evaporated and the crude material immediately purified by flash chromatography (hexane/acetone, 70/30) to give 13.9 mg (63%) of the desired TS dimer ***14β***. mp: Decomposition begins at 189 °C; IR ν (cm^{-1}): 3423 (O—H), 1662 (C═O), 1615 (C═C), 1234 (C—O); ^{1}H NMR (200 MHz, $CDCl_3$, δ ppm): 6.15–6.06 (4H, m, 21-CH and 22-CH), 5.71 (2H, s, 4-CH), 5.74–5.61 (2H, m, 20-CH), 3.70–3.55 (2H, m, 17-CH), 1.25 (3H, s, 19-CH_3), 0.78 (3H, s, 18-CH_3); ^{13}C NMR (200 MHz, $CDCl_3$, δ ppm): 199.1 (C-3), 169.4 (C-5), 132.9 (C-20), 132.2 (C-21), 131.6 (C-22), 125.8 (C-4), 81.3 (C-17), 47.2, 47.0, 46.9, 42.9, 41.2, 39.5, 39.2, 38.8, 35.9, 34.0, 30.3, 22.8, 20.6, 17.8, 11.0; HRMS (ESI+): $(M + H)^+$ calculated for $C_{44}H_{61}O_4$ = 653.4564; found = 653.4561.

5.3.1.5. Preparation of trans, trans,trans-1,6-bis-(17α-hydroxy-4-androsten-3-one-7α-yl)hexatriene (14α).: Following the procedure described for the preparation of dimer **14β** using 7α-(buta-1,3-dienyl)-4-androsten-17α-ol-3-one (**13α**) (22.4 mg, 0.07 mmol) instead of its 17β-hydroxy epimer (**13β**) the titled dimer was obtained with 34% yield (7.2 mg). Purification of the crude material by flash chromatography using a mixture of hexane/acetone, 7/3 gave the desired dimer **14α**. mp: Decomposition begins at 163.8 °C; IR ν (cm^{-1}): 3432 (O—H), 1660 (C═O), 1615 (C═C), 1235 (C—O); ^{1}H NMR (200 MHz, $CDCl_3$, δ ppm): 6.11–6.06 (4H, m, 21-CH and 22-CH), 5.71 (2H, s, 4-CH), 5.71–5.57 (2H, m, 20-

CH), 3.72 (2H, d, J = 5,9 Hz, 17-CH), 1.25 (3H, s, 19-CH_3), 0.70 (3H, s, 18-CH_3); ^{13}C NMR (200 MHz, $CDCl_3$, δ ppm): 199.1 (C-3), 169.2 (C-5), 132.6 (C-20), 132.2 (C-21), 131.7 (C-22), 125.7 (C-4), 79.5 (C-17), 53.8, 47,0, 45.3, 43.2, 42.2, 39.6, 39.4, 38.7, 35.9, 34.0, 30.9, 23.9, 20.6, 17.8, 16.9; HRMS (ESI+): $(M + H)^+$ calculated for $C_{44}H_{61}O_4$ = 653.4564; found = 653.4562.

5.3.1.6. Preparation of trans, trans,trans-1,6-bis-(4-androsten-3,17-dione-7α-yl)hexatriene (14).: Following the procedure described for the preparation of dimer **14β** using the oxidized derivative 7α-(buta-1,3-dienyl)-4-androsten-3,17-dione (**13**) (41.5 mg, 0.12 mmol) the titled dimer **14** was obtained with 77% yield (30.8 mg). This dimer was purified by flash chromatography using a mixture of hexane/acetone, 7/3. mp: Decomposition begins at 175 °C; IR ν (cm^{-1}): 1734 (C═O), 1663 (C═O enone), 1614 (C═C); ^{1}H NMR(200 MHz, $CDCl_3$, δ ppm): 6.15–6.09 (4H, m, 21-CH and 22-CH), 5.73 (2H, s, 4-CH), 5.78–5.63 (2H, m, 20-CH), 1.25 (3H, s, 19-CH_3), 0.91 (3H, s, 18-CH_3); ^{13}C NMR (200 MHz, $CDCl_3$, δ ppm): 219.9 (C-17), 198.8 (C-3), 168.1 (C-5), 132.5 (C-20), 132.3 (C-21), 131.7 (C-22), 126.0 (C-4), 47.6, 47.5, 47.1, 40.7, 39.4, 38.8, 38.6, 35.9, 35.5, 34.0, 30.9, 21.3, 20.3, 17.7, 13.7; HRMS (ESI+): $(M + H)^+$ calculated for $C_{44}H_{57}O_4$ = 649.4251; found = 649.4253.

5.3.1.7. Preparation of 4-(17β-hydroxy-4-androsten-3-one-7α-yl)-3a,4,7,7a-tetrahydro-isobenzofuran-1,3-dione (15).: The steroid derivative 7α-(buta-1,3-dienyl)-4-androsten-17β-ol-3-one (**13β**) (22.3 mg, 0.06 mmol) was dissolved in toluene (0.5 mL) and maleic anhydride was added (31.6 mg, 0.32 mmol). The solution was stirred at reflux for 3 h. Afterwards, the reaction mixture was cooled down and evaporated under reduced pressure. The crude material was purified by flash chromatography (hexane/acetone 7/3) to give 5.2 mg of pure Diels-Alder adduct **15** with 19% yield. mp: 152–154 °C; IR (cm^{-1}): 3415 (O—H), 1845 and 1771 (C═O, anhydride), 1663 (C═O), 1613 (C═C), 1242 (C—O); ^{1}H NMR (200 MHz, $CDCl_3$, δ ppm): 6.03 (2H, br s, 20-CH and 21-CH), 5.77 (1H, s, 4-CH), 3.65–3.50 (2H, m, 17-CH and 25-CH), 3.39 (1H, t, J = 7.8 Hz, 22-CH), 1.30 (3H, s, 19-CH_3), 0.81 (3H, s, 18-CH_3); ^{13}C NMR (200 MHz, $CDCl_3$, δ ppm): 198.7 (C-3), 173.9 (C-23), 172.0 (C-24), 169.8 (C-5), 134.0 (C-21), 128.1 (C-20), 125.6 (C-4), 81.0 (C-17), 46.0, 45.3, 43.4, 42.0, 41.4, 40.9, 39.0, 38.2, 36.1, 35.7, 35.5, 34.5, 34.1, 30.0, 25.2, 24.6, 20.6, 19.0 10.8; HRMS (ESI+): $(M + H)^+$ calculated for $C_{27}H_{35}O_5$ = 439.2479; found = 439.2477.

Supplementary Material

Refer to Web version on PubMed Central for supplementary material.

Acknowledgments

The authors thank the Cancer Research Society (CRS: number 22471) and the Canadian Institutes of Health Research for financial support (CIHR; number 392334). This work was also sponsored by a grant from Aligo Innovation (number 150923), the "*Ministère de l'Économie et de l'Innovation*", Québec government to C. Reyes-Moreno and G. Bérubé, and by the National Institutes of Health Grant ES025767 to I. F. Sevrioukova.

Abbreviations:

BFC	7-benzyloxy-4-(trifluoromethyl)coumarin
CYP3A4	cytochrome P450 3A4
CPA	cyproterone acetate
DHT	dihydrotestosterone
PCa	prostate cancer
TS	testosterone
epiTS	epitestosterone

References

[1]. Nicolaou KC, Montagnon T, Molecules that Changed the World: A Brief History of the Art and Science of Synthesis and its Impact on Society, Wiley-VCH, Weinheim, 2008.

[2]. Rana A, Alex JM, Chauhan M, Joshi G, Kumar R, A review on pharmacophoric designs of antiproliferative agents, Med. Chem. Res 24 (2015) 903–920.

[3]. Nepali K, Sharma S, Sharma M, Bedi PMS, Dhar KL, Rational approaches, design strategies, structure activity relationship and mechanistic insights for anticancer hybrids, Eur. J. Med. Chem 77 (2014) 422–487. [PubMed: 24685980]

[4]. Shaveta S Mishra, P. Singh, Hybrid molecules: the privileged scaffolds for various pharmaceuticals, Eur. J. Med. Chem 124 (2016) 500–536. [PubMed: 27598238]

[5]. Bérubé G, An overview of molecular hybrids in drug discovery, Expet Opin.-Drug Discov 11 (2016) 281–305.

[6]. Bérubé G, Natural and synthetic biologically active dimeric molecules: anticancer agents, anti-HIV agents, steroid derivatives and opioid antagonists, Curr. Med. Chem 13 (2006) 131–154. [PubMed: 16472210]

[7]. Choudhary S, Singh PK, Verma H, Singh H, Silakari O, Success stories of natural product-based hybrid molecules for multifactorial diseases, Eur. J. Med. Chem 151 (2018) 82–97.

[8]. Naha L, Sarker SD, Steroid Dimers: Chemistry and Applications in Drug Design and Delivery, first ed., 2012, p. 440. West Sussex, United Kingdom.

[9]. Sumoto K, Synthetic studies on developments for bioactive new leads of oligovalent symmetrical molecules, Yakugaku Zasshi 140 (2020) 529–541. [PubMed: 32238636]

[10]. Nadal M, Prekovic S, Gallastegui N, Helsen C, Abella M, Zielinska K, Gay M, Vilaseca M, Taulès M, Houtsmuller AB, van Royen ME, Claessens F, Fuentes-Prior P, Estébanez-Perpiñá E, Structure of the homodimeric androgen receptor ligand-binding domain, Nat. Commun 8 (2017) 14388. [PubMed: 28165461]

[11]. Bastien D, Leblanc V, Asselin E, Berube G, First synthesis of separable isomeric testosterone dimers showing differential activities on prostate cancer cells, Bioorg. Med. Chem. Lett 20 (2010) 2078–2081. [PubMed: 20226660]

[12]. Denisov IG, Mak PJ, Grinkova YV, Bastien D, Bérubé G, Sligar SG, Kincaid JR, The use of isomeric testosterone dimers to explore allosteric effects in substrate binding to cytochrome P450 CYP3A4, J. Inorg. Biochem 158 (2016) 77–85. [PubMed: 26774838]

[13]. Millership JS, Shanks ML, Prodrugs utilizing organosilyl derivation: an investigation of the long-term androgenic and myotrophic activities of silyl derivatives of testosterone, J. Pharmaceut. Sci 77 (1988) 116–119.

[14]. Nahara Lutfun, Sarkerb Satyajit D., Turnera Alan B., Synthesis of 17β-hydroxy steroidal oxalate dimers from naturally occurring steroids, Acta Chim. Slov 54 (2007) 903–906.

[15]. Vesper A-R, Lacroix J, Gaudreault RC, Tajmir-Rihai H-A, Bérubé G, Synthesis of novel C2-symmetric testosterone dimers and evaluation of antiproliferative activity on androgen-dependent and –independent prostate cancer cell lines, Steroids 115 (2016) 98–104. [PubMed: 27553724]

[16]. Krstić NM, Bjelaković MS, Dabović MM, Pavlović VD, Thionation of some α,β-unsaturated steroidal ketones, Molecules 15 (2010) 3462–3477. [PubMed: 20657494]

[17]. Krstić NM, Matić IZ, Juranić ZD, Novaković IT, Sladić DM, Steroid dimers—*In vitro* cytotoxic and antimicrobial activities, J. Steroid Biochem. Mol. Biol 143 (2014) 365–375. [PubMed: 24923733]

[18]. Brenner DR, Weir HK, Demers AA, Ellison LF, Louzado C, Shaw A, Turner D, Woods RR, Smith LM, Projected estimates of cancer in Canada in 2020, CMAJ (Can. Med. Assoc. J.) 192 (2020) E199–E205. [PubMed: 32122974]

[19]. Heinlein CA, Chang C, Androgen receptor in prostate cancer, Endocr. Rev 25 (2004) 276–308. [PubMed: 15082523]

[20]. Bastien D, Hanna R, Leblanc V, Asselin E, Bérubé G, Synthesis and preliminary *in vitro* biological evaluation of 7á-testosterone-chlorambucil hybrid designed for the treatment of prostate cancer, Eur. J. Med. Chem 64 (2013) 442–447. [PubMed: 23665800]

[21]. Zhang HJ, Demerseman B, Xi Z, Bruneau C, Ruthenium catalysts for controlled mono-and bis-allylation of active methylene compounds with aliphatic allylic substrates, Adv. Synth. Catal 351 (2009) 2724–2728.

[22]. Dionne P, Ngatcha BT, Poirier D, D-ring allyl derivatives of 17β- and 17α-estradiols: chemical synthesis and ^{13}C NMR data, Steroids 62 (1997) 674–681. [PubMed: 9381515]

[23]. Cheng Y-S, Liu W-L, Chen S, Pyridinium chlorochromate adsorbed on alumina as a selective oxidant for primary and secondary alcohols, Synthesis 3 (1980) 223–224.

[24]. Connon SJ, Blechert S, Recent developments in olefin cross-metathesis, Angew. Chem. Int. Ed 42 (2003) 1900–1923.

[25]. Yee NK, Farina V, Efficient large-scale synthesis of BILN 2061, a potent HCV protease inhibitor, by a convergent approach based on ring-closing metathesis, J. Org. Chem 71 (2006) 7133–7145. [PubMed: 16958506]

[26]. Deslongchamps G, Deslongchamps P, Bent bonds and the antiperiplanar hypothesis as a simple model to predict Diels-Alder reactivity: retrospective or perspective? Tetrahedron 69 (2013) 6022–6033.

[27]. Carmichael J, DeGraff WG, Gazdar AF, Minna JD, Mitchell JB, Evaluation of a tetrazolium-based semiautomated colorimetric assay: assessment of chemosensitivity testing, Canc. Res 47 (1987) 936–942.

[28]. Ford CHJ, Richardson VJ, Tsaltas G, Comparison of tetrazolium colorimetric and [^{3}H]-uridine assays for in vitro chemosensitivity testing, Canc. Chemother. Pharmacol 24 (1989) 295–301.

[29]. Phillips RM, Bibby MC, Double JA, Loadman PM, The relationship between the *in vitro* chemosensitivity of tumor cells and tumor response *in vivo* in an experimental tumor model, Int. J. Cell Clon 9 (1991) 144–154.

[30]. Phillips RM, Bibby MC, Double JA, A critical appraisal of the predictive value of *in vitro* chemosensitivity assays, J. Natl. Cancer Inst 82 (1990) 1457–1468. [PubMed: 2202838]

[31]. Waxman DJ, Attisano C, Guengerich FP, Lapenson DP, Cytochrome P-450 steroid hormone metabolism catalyzed by human liver microsomes, Arch. Biochem. Biophys 263 (1988) 424–436. [PubMed: 3259858]

[32]. Cheng Q, Sohl CD, Yoshimoto FK, Guengerich FP, Oxidation of dihydrotestosterone by human cytochromes P450 19A1 and 3A4, J. Biol. Chem 287 (2012) 29554–29567. [PubMed: 22773874]

[33]. Denisov IG, Baas BJ, Grinkova YV, Sligar SG, Cooperativity in cytochrome P450 3A4: linkages in substrate binding, spin state, uncoupling, and product formation, J. Biol. Chem 282 (2007) 7066–7076. [PubMed: 17213193]

[34]. Finnström N, Bjelfman C, Söderström TG, Smith G, Egevad L, Norlén BJ, Wolf CR, Rane A, Detection of cytochrome P450 mRNA transcripts in prostate samples by RT-PCR, Eur. J. Clin. Invest 31 (2001) 880–886. [PubMed: 11737226]

[35]. Fujimura T, Takahashi S, Urano T, Kumagai J, Murata T, Takayama K, Ogushi T, Horie-Inoue K, Ouchi Y, Kitamura T, Muramatsu M, Homma Y, Inoue S, Expression of cytochrome P450 3A4

and its clinical significance in human prostate cancer, Urology 74 (2009) 391–397. [PubMed: 19501880]

[36]. Kandel SE, Han LW, Mao Q, Lampe JN, Digging deeper into CYP3A testosterone metabolism: kinetic, regioselectivity, and stereoselectivity differences between CYP3A4/5 and CYP3A7, Drug Metabol. Dispos 45 (2017) 1266–1275.

[37]. Krauser JA, Voehler M, Tseng LH, Schefer AB, Godejohann M, Guengerich FP, Testosterone 1β-hydroxylation by human cytochrome P450 3A4, Eur. J. Biochem 271 (2004) 3962–3969. [PubMed: 15373842]

[38]. Choi MH, Skipper PL, Wishnok JS, Tannenbaum SR, Characterization of testosterone 11β-hydroxylation catalyzed by human liver microsomal cytochromes P450, Drug Metab. Dispos 33 (2005) 714–718. [PubMed: 15764715]

[39]. Sevrioukova IF, High-level production and properties of the cysteine-depleted cytochrome P450 3A4, Biochemistry 56 (2017) 3058–3067. [PubMed: 28590129]

[40]. Samuels ER, Sevrioukova IF, Rational design of CYP3A4 inhibitors: a one-atom linker elongation in ritonavir-like compounds leads to a marked improvement in the binding strength, Int. J. Mol. Sci 22 (2021) 8520.

[41]. McCoy AJ, Grosse-Kunstleve RW, Adams PD, Winn MD, Storoni LC, Read RJ, Phaser crystallographic software, J. Appl. Crystallogr 40 (2007) 658–674. [PubMed: 19461840]

[42]. Adams PD, Afonine PV, Bunkóczi G, Chen VB, Davis IW, Echols N, Headd JJ, Hung LW, Kapral GJ, Grosse-Kunstleve RW, McCoy AJ, Moriarty NW, Oeffner R, Read RJ, Richardson DC, Richardson JS, Terwilliger TC, Zwart PH, PHENIX: a comprehensive Python-based system for macromolecular structure solution, Acta Crystallogr. D Biol. Crystallogr 66 (2010) 213–221. [PubMed: 20124702]

[43]. Emsley P, Lohkamp B, Scott WG, Cowtan K, Features and development of coot, Acta Crystallogr. D Biol. Crystallogr 66 (2010) 486–501. [PubMed: 20383002]

[44]. Armarego WLF, Purification of Laboratory Chemicals, Eight Edition, Butterworth-Heinemann, Oxford, 2017, ISBN 9780128054574, p. 1198.

[45]. Still WC, Kahn M, Mitra A, Rapid chromatographic technique for preparative separations with moderate resolution, J. Org. Chem 43 (1978) 2923–2925.

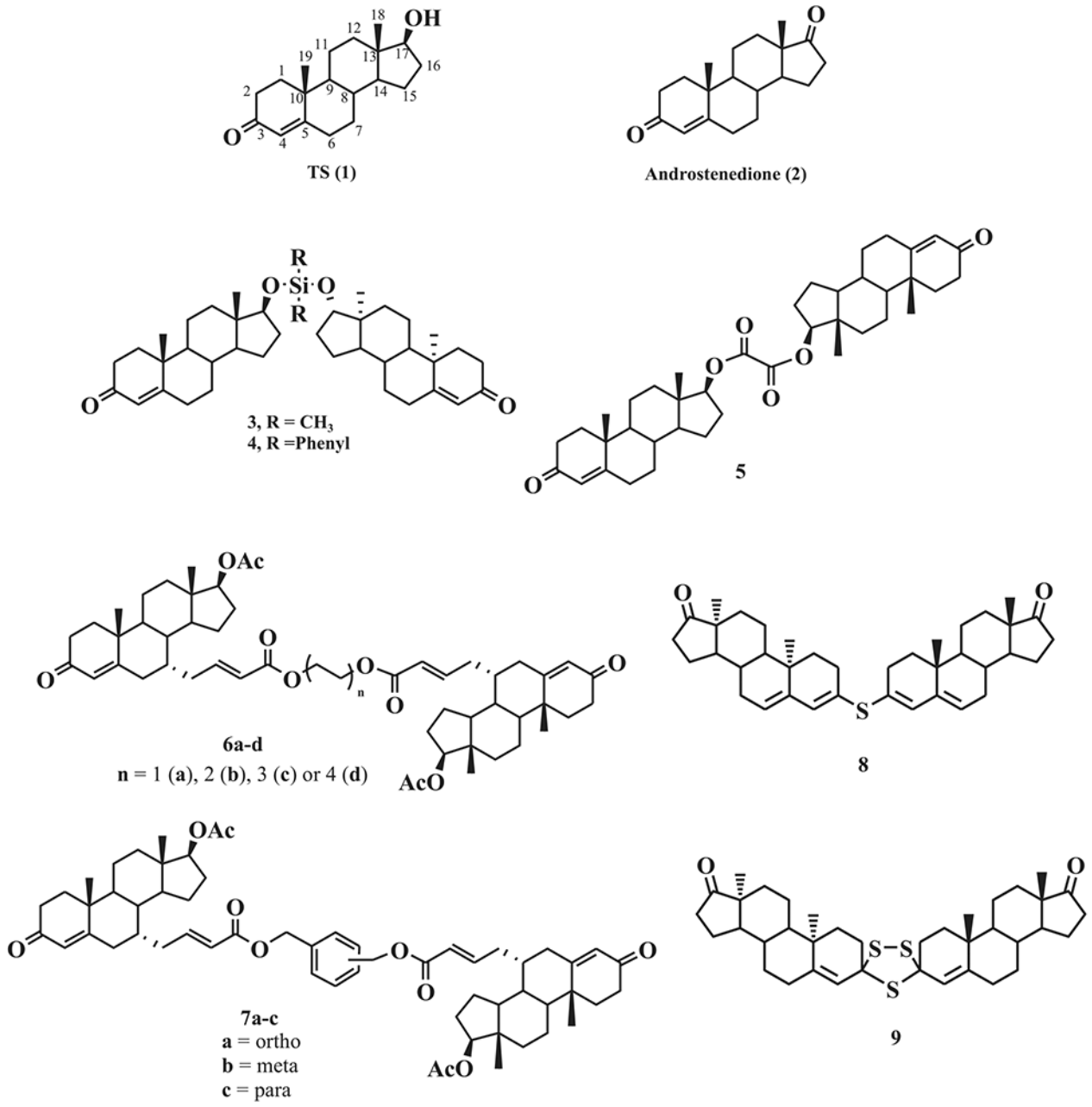

Fig. 1.

TS (**1**) and androstenedione (**2**) with diverse examples of known dimers linked by a silyl ether (**3**,**4**), diester (**5–7**) or sulfur bridge (**8**,**9**).

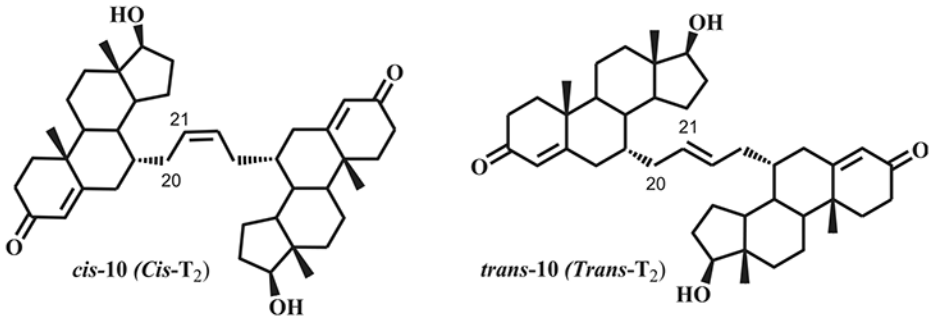

Fig. 2.

Structure of known isomeric TS dimers (*cis*-**10** and *trans*-**10**) linked by a but-2-ene carbon atom chain.

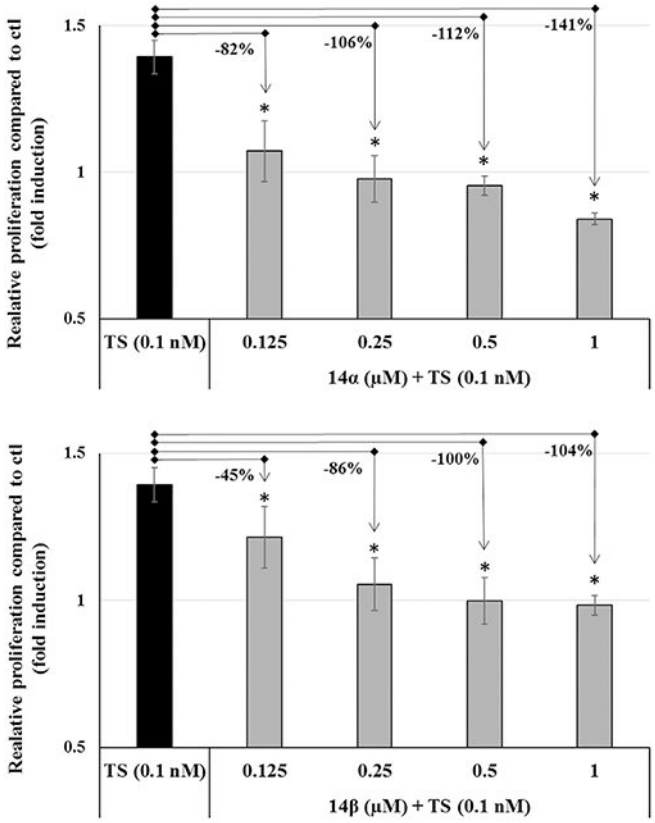

Fig. 3.

Inhibition of TS-induced growth of LNCaP PCa cells by **14α** and **14β** dimers. Cells were cultured for 48 h in DMSO 0.1% (control), TS 0.1 nM alone, or TS 0.1 nM in combination with **14α** and **14β** dimers at different concentrations. Data is expressed as fold induction of cell proliferation compared to control (0.1% DMSO in culture media). Error bars represent ± SEM (n = 3). Statistical analysis: $*p < 0.05$ by two-way ANOVA, Bonferroni's post-test compared to TS.

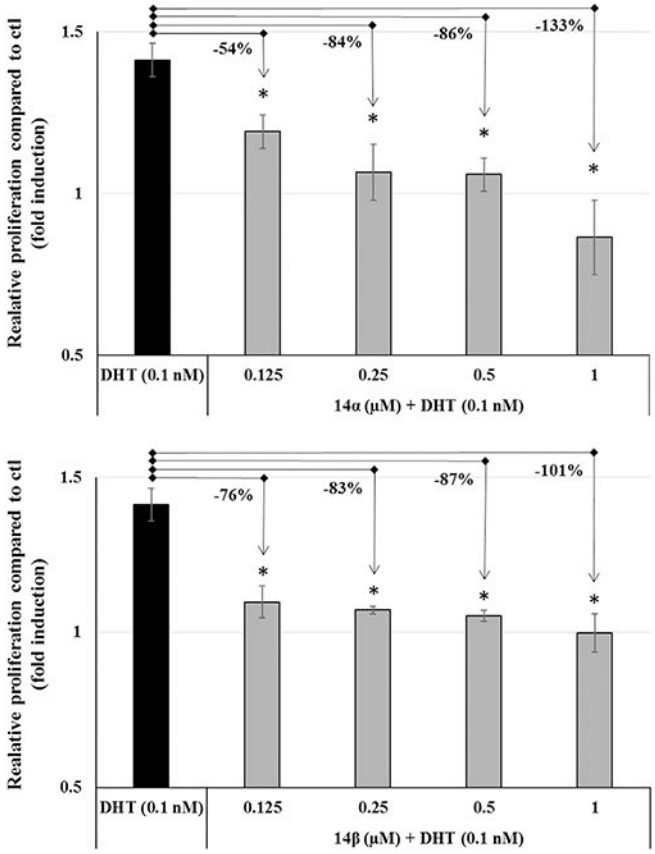

Fig. 4.

Inhibition of DHT-induced growth of LNCaP PCa cells by **14α** and **14β** dimers. Cells were cultured for 48 h in DMSO 0.1% (control), DHT 0.1 nM alone, or DHT 0.1 nM in combination with **14α** and **14β** dimers at different concentrations. Data is expressed as fold induction of cell proliferation compared to control (0.1% DMSO in culture media). Error bars represent ± SEM (n = 3). Statistical analysis: $*p < 0.05$ by two-way ANOVA, Bonferroni's post-test compared to DHT.

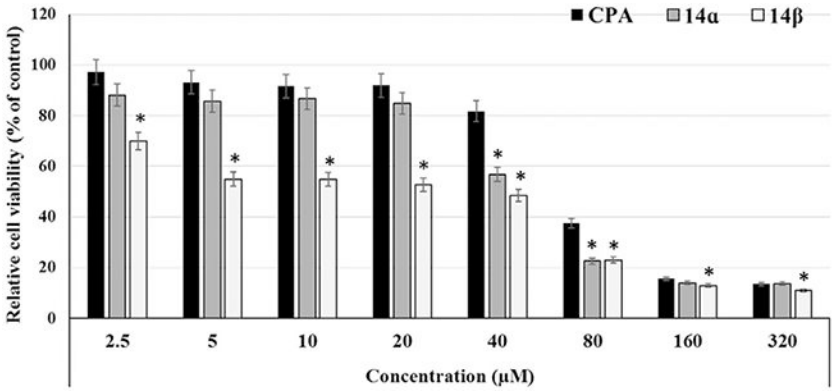

Fig. 5.

Comparative effects of CPA versus **14α** or **14β** dimers on the growth of LNCaP PCa cells. Cells were cultured for 48 h in the presence of DMSO 0.1% (control), and different concentrations of either CPA, **14α** or **14β** dimers. Relative cell viability data is presented as percent of control (0.1% DMSO in culture media; color coding indicated). Error bars represent ± SEM (n = 3). Statistical analysis: *$p < 0.05$ by two-way ANOVA, Bonferroni's post-test compared to each CPA concentration.

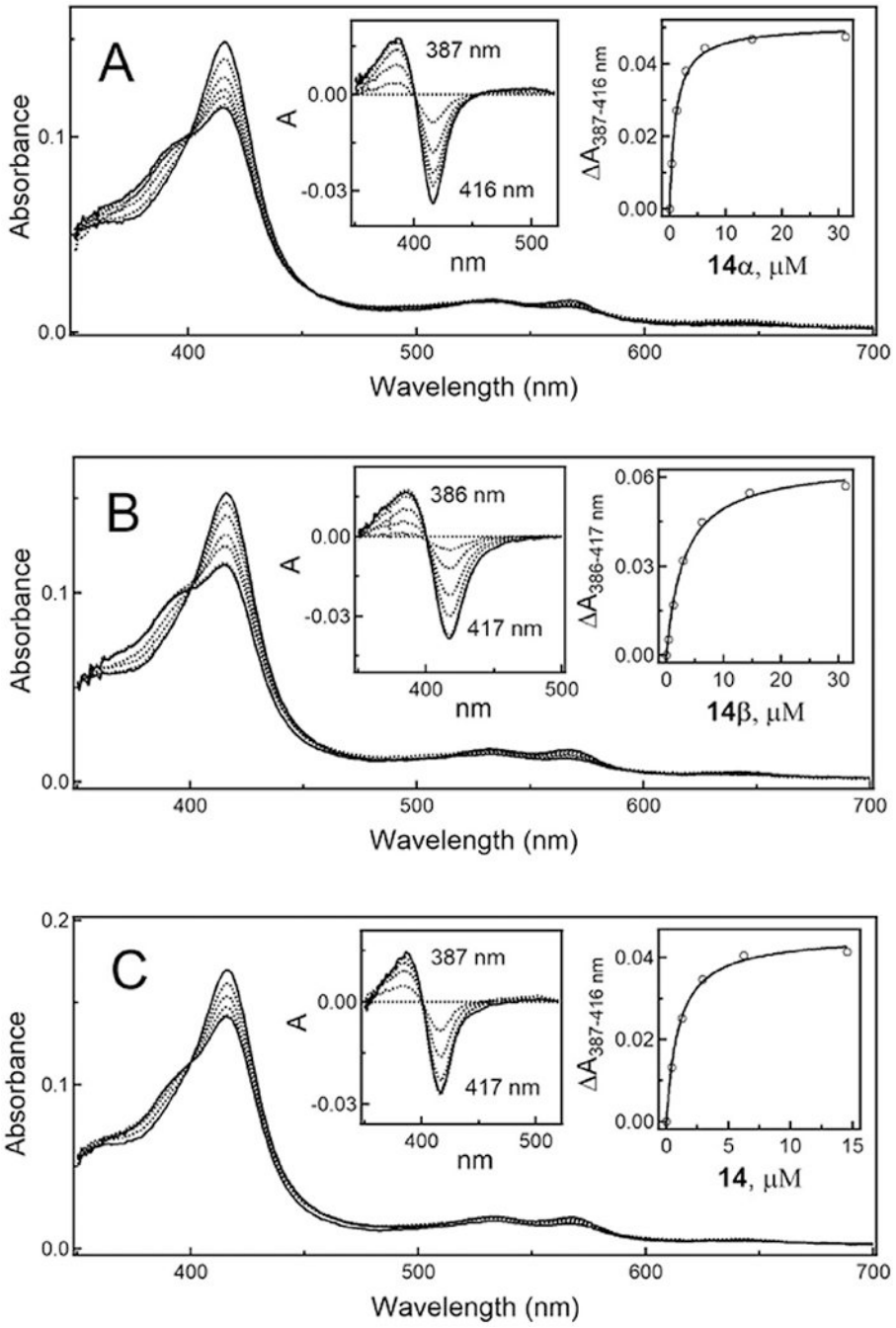

Fig. 6.

A-**C**, Spectral changes in CYP3A4 induced by TS dimers **14α**, **14β** and **14**, respectively. Absorbance spectra of 2 μM CYP3A4 at different ligand concentrations were recorded in 0.1 M phosphate buffer, pH 7.4, at room temperature. Left insets are the difference spectra; right insets are titration plots with hyperbolic fittings. The derived K_d values are given in Table 2.

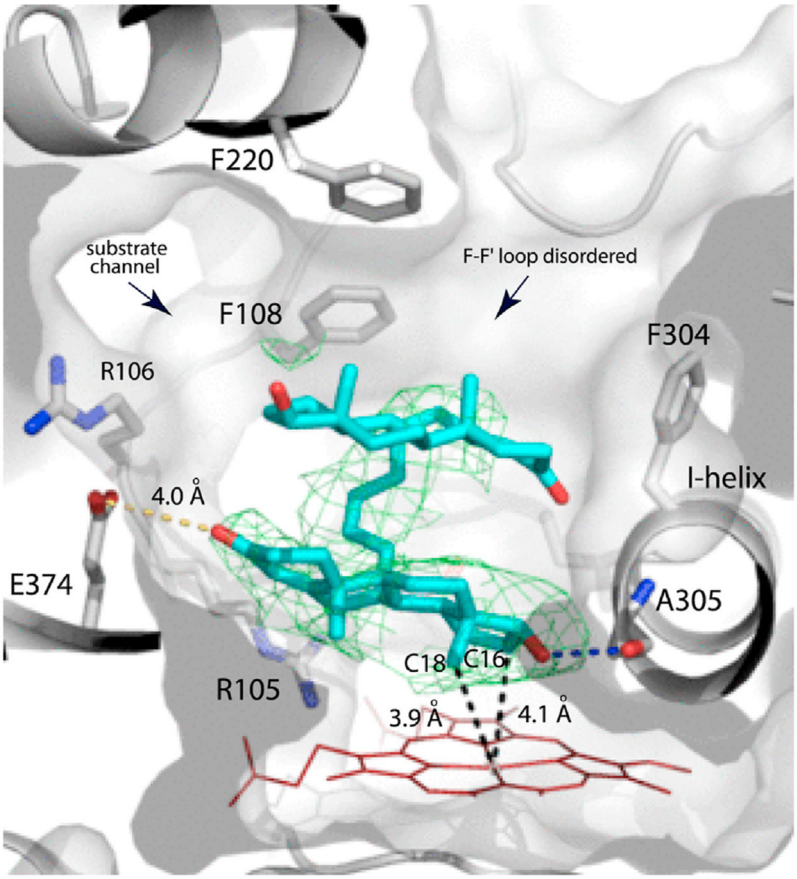

Fig. 7.

Crystal structure of CYP3A4 bound to the TS dimer *cis*-**10** (shown in cyan sticks). Sterol ring closest to the heme is well-defined and H-bonds via the hydroxyl group to the carbonyl oxygen of Ala305. Carbon atoms closest to the heme iron are labeled. The catalytic cavity is more open and, in addition to the substrate channel, can be accessed through the opening created by disorder in the F–F′ loop (indicated by arrows). Green mesh is polder omit map contoured at 3 σ level.

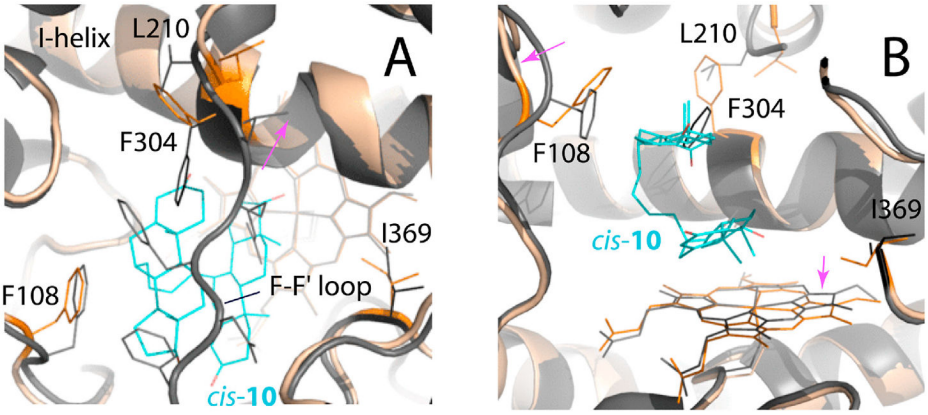

Fig. 8.

Conformational changes in CYP3A4 induced by *cis*-**10**. **A** and **B**, Top and side views at the active site of ligand-free (4I3Q structure; in black) and *cis*-**10** bound CYP3A4 (in beige and orange), respectively. Association of *cis*-**10** triggers displacement of the I-helix and the heme plane (by 1.2 and 0.7 Å respectively), rotameric switch in Phe304, positional shift in the Phe108-centered loop (by 2.9 Å), and disorder in the F–F′ fragment (residues 211–215). Movements of structural elements are indicated by arrows.

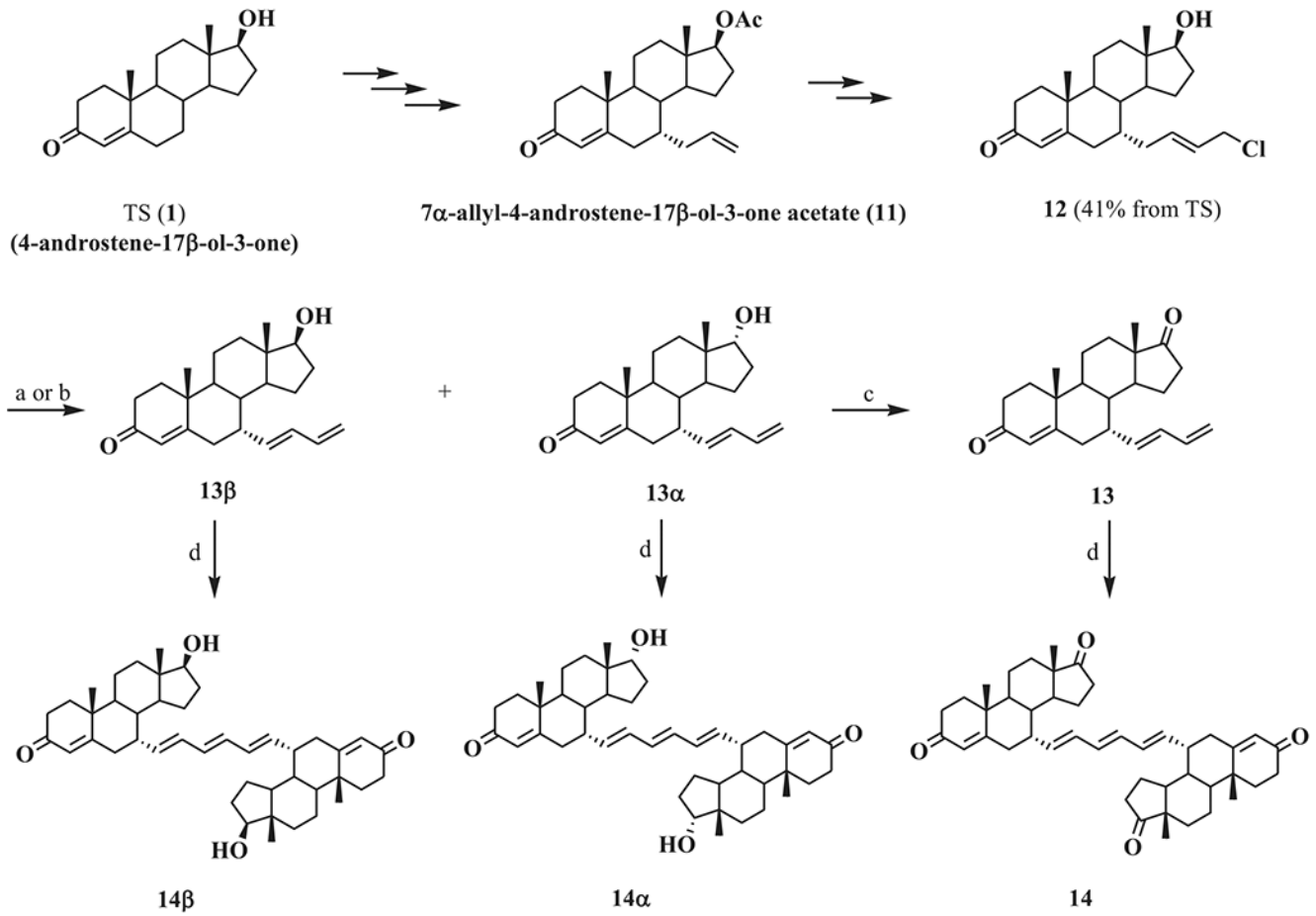

Scheme 1. Reagents and conditions:

(a) $[Ru(C_5Me_5)(MeCN)_3)]$ $[PF_6]$, CS_2CO_3, CH_3CN, N_2, 48 h (**13β**, 66%); or (b) $[Ru(C_5Me_5)(MeCN)_3)]$ $[PF_6]$ (lot #MKCK1977), CS_2CO_3, CH_3CN, N_2, 48 h (**13β**, 17% and **13α**, 18%); (c) Mixture of **13α** and **13β**, pyridinium chlorochromate, Al_2O_3, CH_2Cl_2, 2.5 h (**13**, 63%); (d) Relevant diene, Hoveyda-Grubb's catalyst 2nd generation, CH_2Cl_2, N_2, 36 h (**13β → 14β**, 63%; **13α → 14α**, 34%; **13 → 14**, 77%).

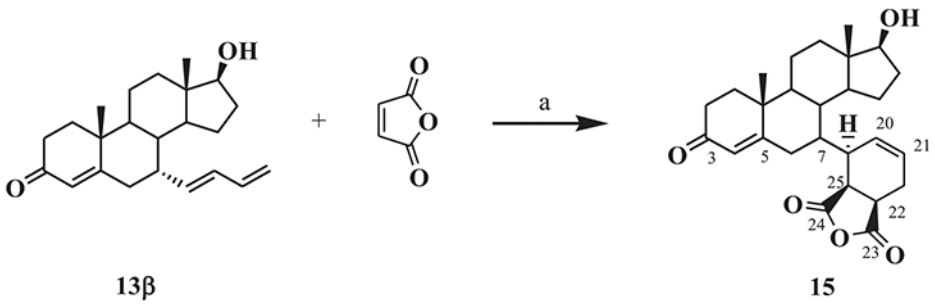

13β 15

Scheme 2. Reagents and conditions:

(a) Diene **13β**, maleic anhydride, toluene, 3 h at 110 °C (19% yield).

Table 1

Antiproliferative activity of novel TS dimers (compound **14α** and **14β**) and androstenedione dimer (compounds **14**), their respective precursors (**13α, 13β** and **13**), the Diels-Alder adduct **15** and CPA on androgen-sensitive (LNCaP) and androgen-insensitive (PC3 and DU145) human prostate adenocarcinoma cell lines.

Compound	IC_{50} (μM)[a]		
	LNCaP (AR^+)	PC3 (AR^-)	DU145 (AR^-)
13α	16.6	31.5	23.8
13β	28.8	34.1	29.0
13	33.5	51.7	21.3
14α	37.1	44.5	21.4
14β	12.0	13.6	14.4
14	72.7	29.0	53.6
15	130.6	62.5	86.5
[b]CPA	59.6	56.9	50.7

[a]Inhibitory concentration (IC_{50}) is concentration of drug inhibiting cell growth by 50%.

[b]Cyproterone acetate.

Table 2

Interaction of new TS dimers (**14α** and **14β**), androstenedione dimer (**14**) and previously produced *cis*-**10** and *trans*-**10** with isolated recombinant CYP3A4.

Compound	K_d [a] μM	high spin %	IC_{50} [b] μM
14α	1.6 ± 0.3	46 ± 3	22 ± 2
14β	5.5 ± 0.7	49 ± 3	1.2 ± 0.2
14	1.4 ± 0.2	36 ± 2	3.6 ± 0.4
cis-**10** [c]	0.37 ± 0.3	99 ± 1	0.8 ± 0.1
trans-**10** [c]	7.1 ± 0.5	65 ± 4	6.5 ± 0.5

All values represent an average of three measurements with a standard deviation.

[a] Spectral dissociation constant.

[b] Half-inhibitory concentration for the BFC debenzylase activity of CYP3A4.

[c] Described previously [11,12].